199 Landslide Hazard: Risk Zonation and Impact Wave Analysis for the Bumbuma Dam—Sierra Leone

Battaglia Daniele, Strozzi Tazio, and Bezzi Alberto

Abstract

The Bumbuna Dam is located along the Seli River in northern Sierra Leone. The dam creates a 37 km long reservoir for a total volume of 430 Mm^3 and a maximum depth of 80 m. The area is vegetated by a thick savanna forest. We evaluated the landslide hazard and risk conditions along the reservoir banks and its surrounding areas based on expert photointerpretation of laserscan data, optical satellite imagery, differential Synthetic Aperture Radar (SAR) interferometry, and field work. Past landslides features, mainly debris slides of regolite soil over the bedrock, were identified from photointerpretation and part of them were verified on field. Slope statistics of the recognized features supported with data from events near the dam site were used to determine the hazard classes along the reservoir area. Risk zonation was based on a weighted criteria approach taking into account three main factors: the hazard class, the altitude above the reservoir and the travel distance to the dam of the impact wave. A reference landslide was defined from the statistical distribution of existing landslides and the amplitude of the impact wave at the dam site was calculated on the base of published formulas. Results indicate that no overtopping of water above the dam crest is expected.

Keywords

Bumbuna dam • Landslide • Risk analysis • Impact wave

199.1 Introduction

The Bumbuna Dam (Lat: 9.072032, Long: -11.723153) is located along the Seli River in Northern Sierra Leone (Fig. 199.1). It operates a reservoir that, at the maximum level, is 37 km long and 80 m deep, for a total volume of 430 millions of cubic meters of water. Dam construction started in the'80 and it was completed in 2009 after a long interruption due to a civil war.

The reservoir extends in a region with a thick vegetation cover and few point of access: there are no roads and foot trails are the only connections between the villages.

During dam construction concern was raised about the occurrence of landslides in the reservoir that could produce impact waves able to overtop the dam crest and damage the powerhouse located at the base of dam and the villages downstream. This paper describes the investigation and analysis conducted to evaluate the landslides hazard and risk in the reservoir area and to estimate the magnitude of a landslide induced wave at the dam site.

Due to the very difficult access condition the study was based mostly on remote sensed data which included high accuracy topographic maps and orthophoto obtained from laserscan survey, optical satellite images, and satellite SAR interferometry. Field surveys focused on the verification of the most relevant remote sensed features, the study of past

B. Daniele (✉)
Studio Georisk, Via Stelvio 20, 20844 Triuggio Italy
e-mail: dbattaglia@georisk.it

S. Tazio
Gamma Remote Sensing AG, Worbstrasse 225, 3073 Gümligen Switzerland
e-mail: strozzi@gamma-rs.ch

B. Alberto
Studio Pietrangeli, Via Del Cicerone 28, 00193 Rome Italy

G. Lollino et al. (eds.), *Engineering Geology for Society and Territory – Volume 2*,
DOI: 10.1007/978-3-319-09057-3_199, © Springer International Publishing Switzerland 2015

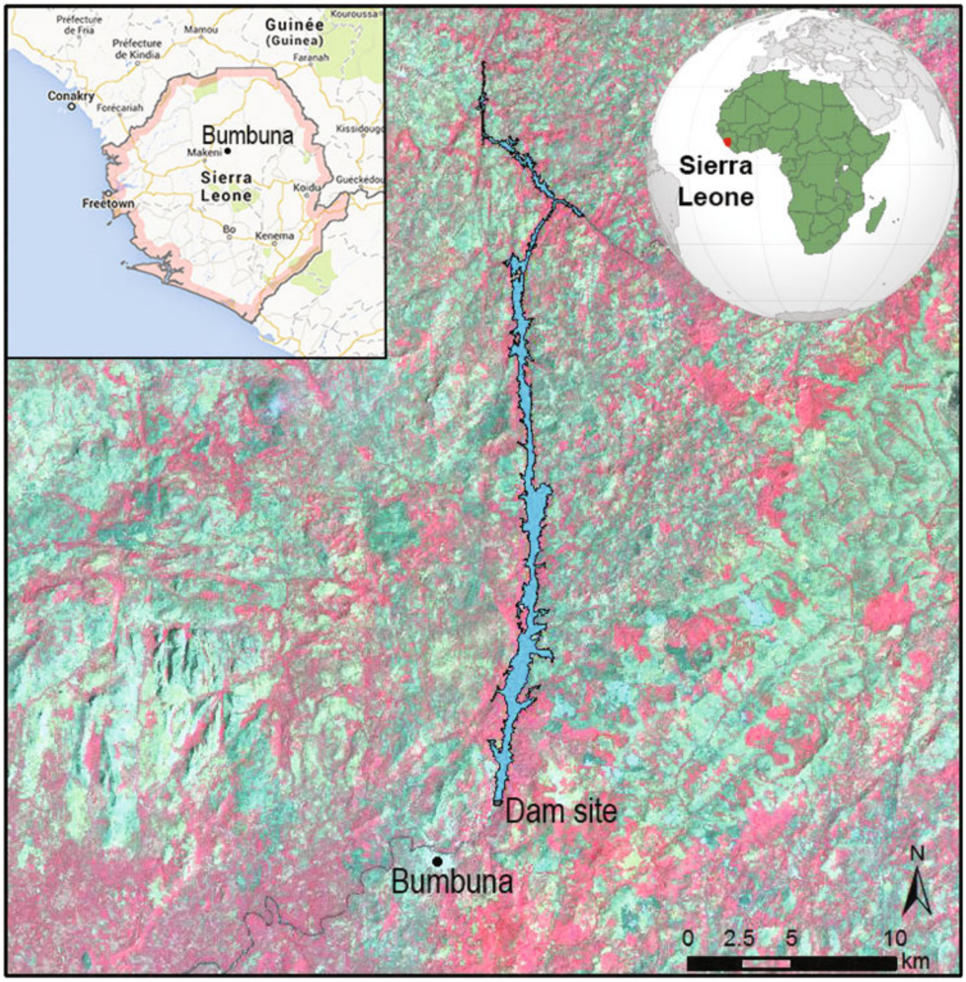

Fig. 199.1 Dam site and reservoir extension (*cyan area*) on Landsat 2002 infrared image

landslides occurred close to the dam site and the periodic inspection of reservoir banks during and after the reservoir impounding.

199.2 Geomorphological and Geological Setting

Topography in the study area ranges between 150 and 640 m above sea level: the highest and lowest altitudes are found in the southern area close to the dam site where the Seli river cross the western portion of the Sula mountains.

The relief morphology is defined by rounded crest zones with gentle slopes and ample flat areas. Valley side are gentle with inclinations usually lower than 40°, slopes are regular in shape and with few changes in slope angle and direction from the top down to the base. Valley floors can be subdivided in two types: the main valleys, produced by Seli and Mawoloko River, which are characterized by flat plains 150–300 m wide, and secondary valleys which have narrow floor and a V shape, with some flat plains irregularly distributed along their length.

The geology of the area consists of Precambrian granites of the Western African Shield and of amphibolites of the Sula Mountain Greenstone Belt (Wilson and Marmo 1958). Rock outcrops are rare and they occur along the hill tops, the secondary valley floors and the Seli river banks. The bedrock is usually covered by residual soils (laterite) produced by in situ weathering, whose thickness can vary from few meters to tens of meters.

199.3 Data

Geomorphological features of past landslide events have been identified through expert photointerpretation of 5 m contour maps obtained by laserscan survey integrated with high resolution ortophotos (0.2 m/pixel).

Landslides deposits have been defined mainly by the geometry of the contour lines, which usually show peculiar irregularities, such as widening or outward deflection of contiguous lines. Upslope of the deposits a depletion zone (Landslide head) and a landslide scarp were frequently observed. The confidence of the interpretation was also recorded. Landslide deposits cover only 4 % of the area and they have on average extension in the range of 6–8000 m^2. No evidence of major mass movements was recognized.

SRTM data (Farr et al. 2007) showed that the stream network was structurally controlled by tens to hundreds of kilometers long lineaments (faults and major joints). Land-use and rock outcrops position was obtained from supervised classification of Landsat images.

Interferometric analysis of 7 satellite SAR images recorded between January 2007 and April 2008 was performed in order to identify signs of active ground movements. ALOS PALSAR data were used because L-band (1.3 GHz, 23.5 cm wavelength) has the capability to achieve fairly coherent interferograms also over vegetated areas (Strozzi et al. 2005).

The analysis was performed on 8 pairs of SAR images with a time interval ranging from a minimum of 46 days to a maximum of 368 days. Signal decorrelation in the vegetated resulted high, but fairly satisfactory phase interferograms were obtained comparing dry seasons images. In general, no major signals related to displacement were detected around the reservoir and on the catchment area. Small size landslide (e.g. with a dimension of few pixels) could not be identified on the PALSAR interferograms due to the SAR pixel size of about 20 m and the need to have a certain number of coherent pixels in order to interpret the interferometric phase.

Reconnaissance surveys were accomplished to verify on field, with spot sampling, the existence and state of the geomorphological features identified from photointerpretation. Surveys were performed in 2008–2009: before, during and after the first impounding of the reservoir. Field work was crucial to defined the failure processes affecting the area and to understand the soil/bedrock relationships.

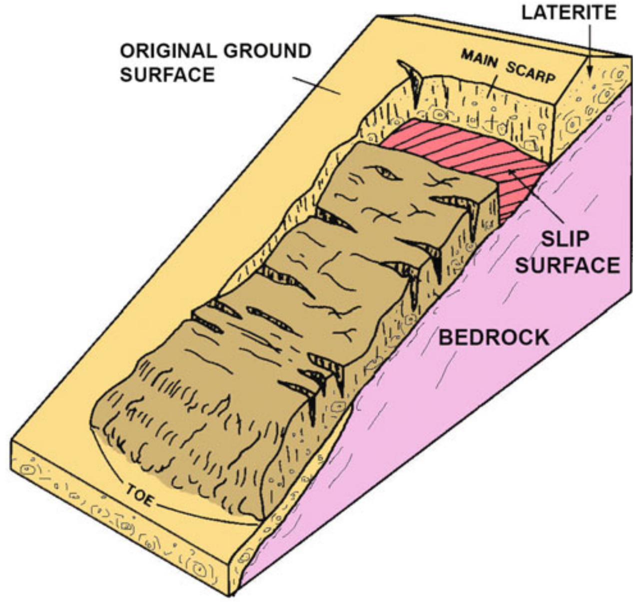

Fig. 199.2 Debris slide of laterite soil over the bedrock (modified from Varnes 1978)

199.4 Landslides Types

Landslides in the Bumbuna catchment are almost entirely constituted by debris slides (Varnes 1978) of laterite soils over the granitic rockhead. The slide occurs along preexisting sheet joints sub-parallel to the surface topography. A typical feature is illustrated in Fig. 199.2: the movement take place along a slip surface (Fig. 199.3) parallel to the slope which is bordered upward by a main scarp developed from a series of tension cracks. Laterally the slide is bounded

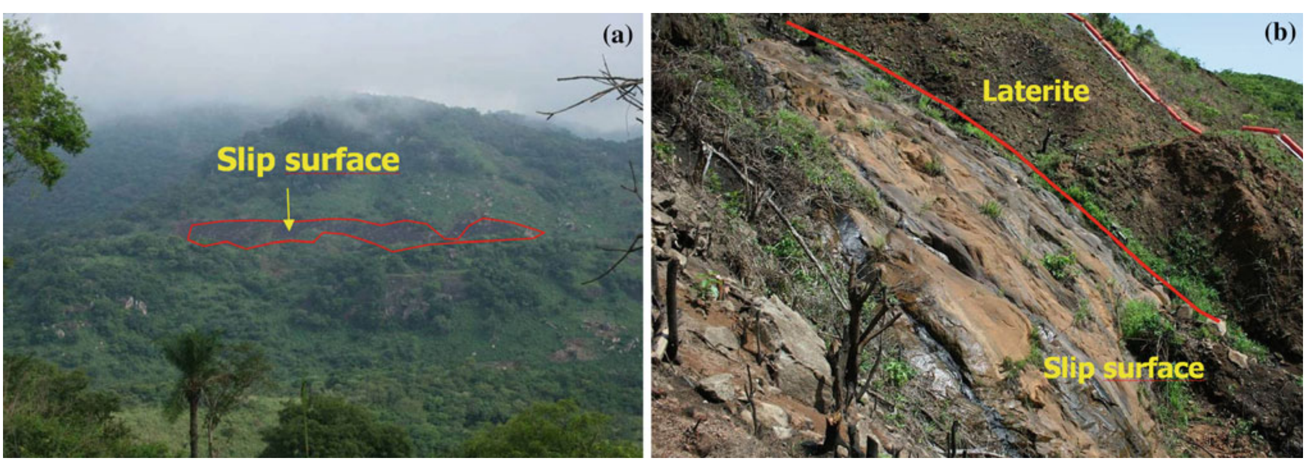

Fig. 199.3 Debris slides on bedrock along planar surfaces **a** panoramic view **b** detail

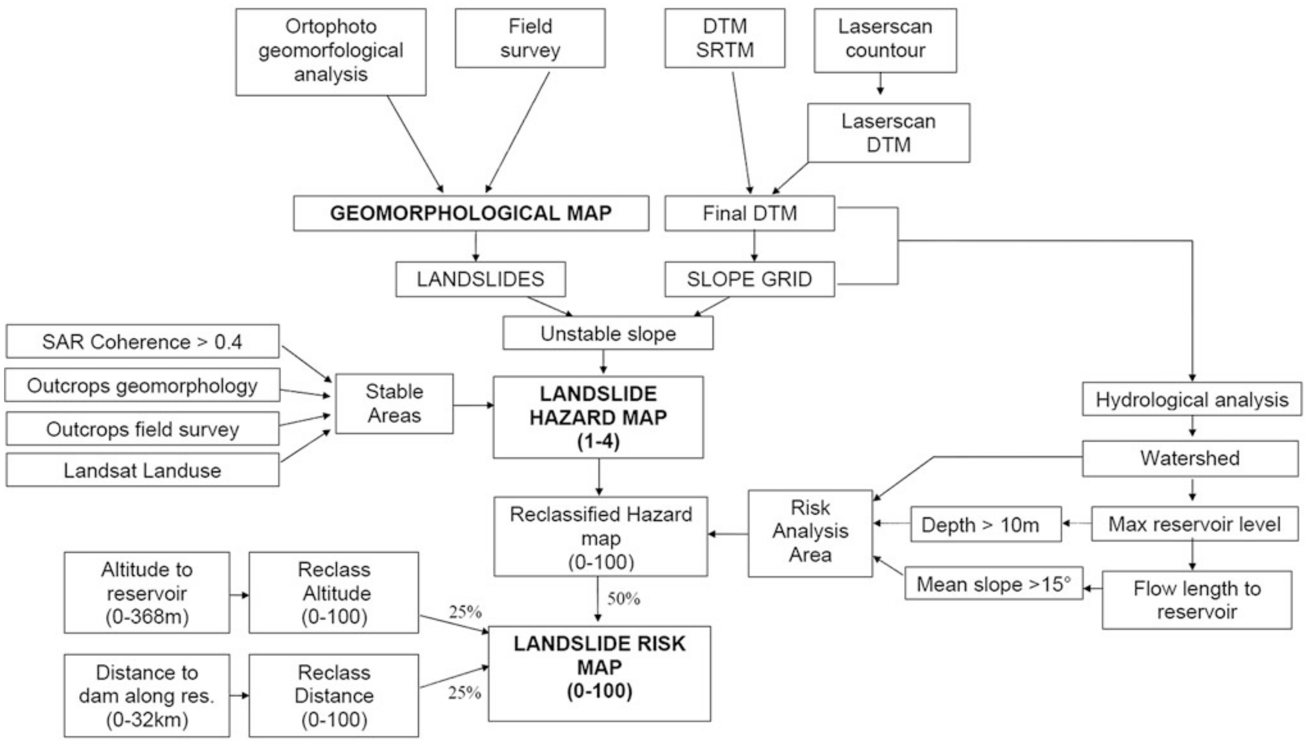

Fig. 199.4 Flow chart for definition of landslide hazard and risk maps

Table 199.1 Hazard classes from slope angle

Hazard class		Slope angle	Description
1	Very low hazard	0–20°	Stable areas
2	low hazard	20–30°	Moderately stable areas
3	Medium hazard	30–40°	Potentially unstable areas
4	High hazard	40–90°	Unstable areas

by vertical and continuous fissures that separate the stable ground from the sliding mass. The landslide body is constituted by a mix of laterite, sandy soil and rock corestones. The event is usually sudden and triggered by the intense precipitations occurring during the rainy season (recorded up to 150 mm/d and 700 mm/month). The rate of movement ranges from rapid to very rapid (from meters/day to meters/sec) and the soil mass often turns into a mud or debris flow.

199.5 Hazard and Risk Zonation

The sequence of analysis used to calculating the hazard and risk map in a GIS environment is illustrated in the flow chart of Fig. 199.4.

Landslide hazard was defined considering the slope angle as the main instability factor. Statistics of the slope angles inside landslide features identified from photointerpretation were extracted with zonal analysis. Results indicate that the mean slope of landslide debris (body) is of 20°, whereas the mean slope of depletion (head) zones is of 30°.

Field evidence, backanalysis of existing landslides and literature data (Lambe 1996) indicated that the residual soil could be subject to failure when saturated on slopes steeper than 30°. Hazard maps at the scale 1:10000 were produced for the whole reservoir area on the base of the scheme indicated in Table 199.1.

Very low hazard conditions were assumed for rock outcrops and areas with high phase coherence identified from SAR interferometry.

Risk maps were produced considering the Bumbuna dam as the single vulnerable element. Numerical rating of contributing factors method (Varnes 1984; van Westen 1993) was chosen for the analysis and the risk was derived from the weighted sum of three normalized factors. The first was the Landslide Hazard which would count for half of the total risk. The second factor was the height above the reservoir, which represents the potential energy of the landslide and would count for a quarter of the total risk. The last factor was the distance that the impact wave would travel along the reservoir to reach the dam. It was obtained calculating first the distance to the dam of the reservoir banks, and then the distance to the reservoir of the valley sides along the landslide direction of movement. The third factor would count for a quarter of the total risk. Final landslide risk map (Fig. 199.5) indicate that 70 % of the area is subject to very or low risk, 28 % to medium risk and only 2 % to high risk.

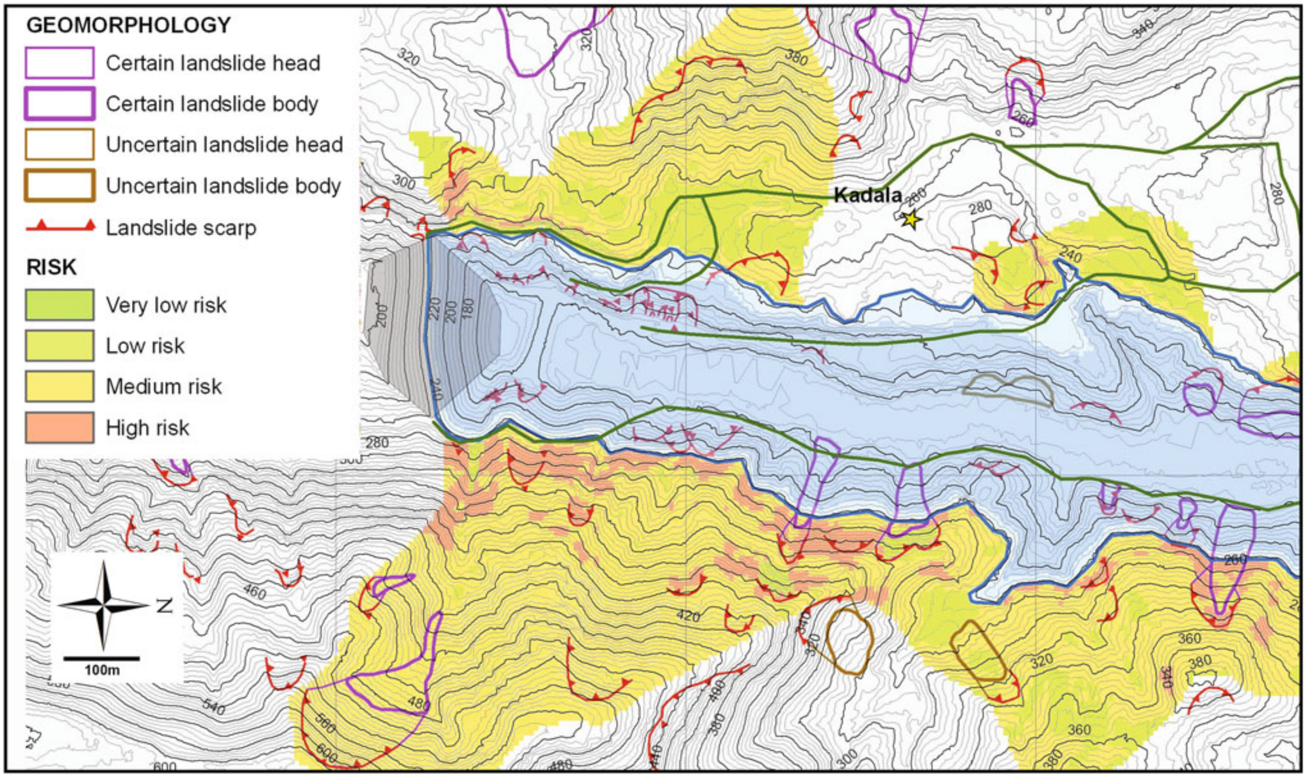

Fig. 199.5 Detail of the final risk map at the dam site

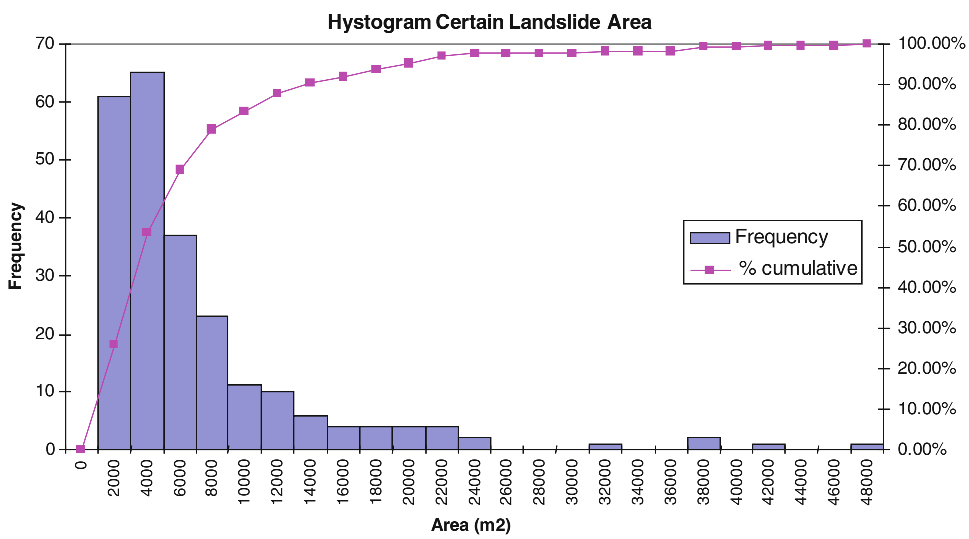

Fig. 199.6 Histogram of certain landslide areas obtained from photointerpretation

199.6 Impact Wave Analysis

For impact wave analysis a maximum expected event (reference landslide) was statically defined on the base of characteristics of the certain landslides identified from photointerpretation. The reference landslide area was considered equal to 20,000 m^2, which correspond to the 95 % percentile of the statistical distribution of the recognized features (Fig. 199.6). The other dimensions were estimated from field evidence: it was considered a length of 200 m, a width of 100 m and a mean depth of the sliding plane of 5 m for a total volume of 10,000 m^3.

Risk maps showed that most of the high risk area were located along or close to the reservoir bank slopes, therefore it was assumed that the drop height of the landslide would be of 30 m for a travel length of 50 m. According to Slingerland and Voight (1979), the impact velocity (Vi) in the reservoir was estimated in 16.8 m/s (60 km/h).

The landslide-generated impulsive wave was calculated from the empirical formulations of Heller (2008), Heller et al. (2009). The author provides a set of equations to forecast the impulse wave characteristics at the impact point and at the distance together with solutions to calculate the wave run-up on a sloping surface, such as the dam upstream face.

Results showed that the expected run up of an impulse wave generated by the reference landslide impacting the reservoir ranges from 1.7 to 2.8 m, therefore the available freeboard of 3.8 m at the dam crest is adequate to avoid the dam overtopping.

199.7 Conclusions

Risk analysis indicated that medium to high risk conditions exists on few areas along the Bumbuna reservoir, but the maximum expected landslide event is not likely to produce impact waves able to overtop the dam crest.

In 2009–2010, during reservoir impounding, no anomalous wave have been observed and inspections of the lake banks revealed the occurrence of only few failures with volumes of the order of hundreds of m^3, much lower than the reference landslide.

Installation of reflective SAR targets have been planned for interferometric monitoring of reservoir slopes in remote areas together with the installation of optic targets for topographic monitoring of the highest risk areas located close to the dam site.

References

Farr TG, Rosen PA, Carol E, Crippen R, Duren R, Hensley S, Kobrick M, Paller M, Rodriguez E, Roth L, Seal D, Shaffer S, Shimada J, Umland J, Werner M, Oskin M, Burbank D, Alsdorf D (2007) The shuttle radar topography mission, Rev Geophys 45: RG2004. doi:10.1029/2005RG000183

Heller V (2008) Landslide generated impulse waves - Prediction of near field characteristics. In: Minor HE (ed) VAW Mitteilung, vol 204. ETH Zurich, Zurich

Heller V, Hager WH, Minor HE (2009) Landslide generated impulse waves in reservoirs—basics and computation. In: Boes R (ed) VAW Mitteilung, vol 211. ETH Zurich, Zurich

Lambe PC (1996) Landslide investigation and mitigation, special report 247—transportation research board, National Academy Press, Washington

Slingerland RL, Voight B (1979), Occurrences, properties and predictive models of landslide generated impulse waves. In: Voight B (ed) Rockslides and avalanches, vol 2, Elsevier, Amsterdam, pp 317–397

Strozzi T, Farina P, Corsini A, Ambrosi C, Thüring M, Zilger J, Wiesmann A, Wegmüller U, Werner C (2005) Survey and monitoring of landslide displacements by means of L-band satellite SAR interferometry. Landslides 2(3):193–201. doi:10.1007/s10346-005-0003-2

Van Westen CJ (1993) Application of Geographical information system to landslide hazard zonation. ITC Publication number 15, Enschede

Varnes DJ (1978) Landslide analysis and control, special report 176 transportation research board. National Academy of Sciences, Washington

Varnes DJ (1984) Landslide hazard zonation: a review of principles and practice. Unesco, Paris

Wilson NW, Marmo V (1958), Geology, Geomorphology and Mineral resources of the Sula mountains, geological survey of Sierra Leone Bulletin 1